

## Application of statistics to CPT-based parameter selection

Lengkeek, H.J.; Jonkman, S. N.; Hauth, M.

**Publication date**

2022

**Document Version**

Final published version

**Published in**

Proceedings of the 20th International Conference on Soil Mechanics and Geotechnical Engineering

**Citation (APA)**

Lengkeek, H. J., Jonkman, S. N., & Hauth, M. (2022). Application of statistics to CPT-based parameter selection. In M. Jaksa, & M. Rahman (Eds.), *Proceedings of the 20th International Conference on Soil Mechanics and Geotechnical Engineering* International Society for Soil Mechanics and Geotechnical Engineering. <https://www.issmge.org/publications/publication/application-of-statistics-to-cpt-based-parameter-selection>

**Important note**

To cite this publication, please use the final published version (if applicable).  
Please check the document version above.

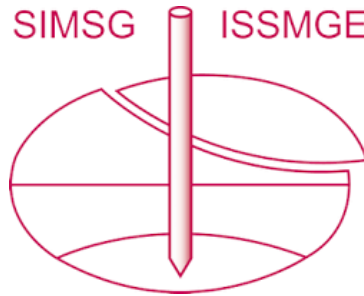
**Copyright**

Other than for strictly personal use, it is not permitted to download, forward or distribute the text or part of it, without the consent of the author(s) and/or copyright holder(s), unless the work is under an open content license such as Creative Commons.

**Takedown policy**

Please contact us and provide details if you believe this document breaches copyrights.  
We will remove access to the work immediately and investigate your claim.

# INTERNATIONAL SOCIETY FOR SOIL MECHANICS AND GEOTECHNICAL ENGINEERING



*This paper was downloaded from the Online Library of the International Society for Soil Mechanics and Geotechnical Engineering (ISSMGE). The library is available here:*

<https://www.issmge.org/publications/online-library>

*This is an open-access database that archives thousands of papers published under the Auspices of the ISSMGE and maintained by the Innovation and Development Committee of ISSMGE.*

*The paper was published in the proceedings of the 20<sup>th</sup> International Conference on Soil Mechanics and Geotechnical Engineering and was edited by Mizanur Rahman and Mark Jaksa. The conference was held from May 1<sup>st</sup> to May 5<sup>th</sup> 2022 in Sydney, Australia.*

## Application of statistics to CPT-based parameter selection

### Statistique appliquée à la selection de paramètres à partir d'essais CPT

**H.J. Lengkeek**

*Delft University of Technology, Delft, The Netherlands, h.j.lengkeek@tudelft.nl*  
*Witteveen+Bos, Deventer, The Netherlands*

**M. Hauth & S.N. Jonkman**

*Delft University of Technology, Delft, The Netherlands*

**ABSTRACT:** The derivation of representative values for geotechnical parameters accounts for the various sources of uncertainty which are addressed at different stages of the determination process. A comprehensive flow chart for the determination of constitutive model parameters from site tests is proposed. The authors first consider a straightforward methodology to quantify the inherent uncertainty of variables measured from a CPT. An automated framework is then applied to merge outcomes from several transformation functions into a single combined output. This result can be subsequently updated with expert judgment or with direct measurements from laboratory tests using a Bayesian approach. When applied to the friction angle, a reduction of the posterior updated representative standard deviation is observed.

**RÉSUMÉ :** Le calcul des valeurs représentatives des paramètres géotechniques doit tenir compte des diverses sources d'incertitude qui sont abordées à différentes étapes du processus de détermination. Un diagramme de flux complet est proposé pour déterminer les paramètres de modèles constitutifs à partir d'essais in-situ. Les auteurs présentent d'abord une méthodologie directe pour quantifier l'incertitude intrinsèque des grandeurs mesurées à partir d'un essai CPT. Un système automatisé est ensuite utilisé pour fusionner les réponses provenant de plusieurs fonctions de transformation en un résultat unique. Avec une approche Bayésienne, l'expertise de l'utilisateur ainsi que des observations directes provenant de tests en laboratoire peuvent servir à mettre à jour le résultat précédemment déterminé. Lorsque ce processus est appliqué à l'angle de frottement, on observe une réduction de son écart-type représentatif a posteriori.

**KEYWORDS:** Automated parameter determination (APD); Graph theory; Cone penetration test (CPT); Spatial variation; Bayesian updating.

## 1 INTRODUCTION

In early stages of a project only limited data is available, mostly consisting of a few CPTs in the area. The geotechnical parameters are often estimated from existing correlations, although the availability and proper selection of correlations can be an issue. In later stages of the project more laboratory tests and CPTs become available. That will reveal other challenges, such as assessing the spatial variation and translating this to a representative value used for design. Although codes and guidelines exist on this topic (see below), the practical application still requires better clarity and guidance.

Uncertainty in geotechnical parameter selection has been addressed for many years (Kulhawy 1992; Phoon 2016; Phoon and Kulhawy 1999a; Phoon and Kulhawy 1999b; Schneider and Schneider 2012; Uzielli et al. 2006). This first type of uncertainty stems from the aleatory nature of soil, in contrast to manufactured materials. The geology of the soils may be taken into account to reduce this type of uncertainty. The second type is the epistemic uncertainty, the safety concepts and implementation in design standards (Ching et al. 2020; Hicks and Nuttall 2012; Orr 2016; Prästings et al. 2019). Furthermore, the complexity of random fields and new insights from numerical simulations are also of importance (Elkateb et al. 2003; Hicks et al. 2019; Qi and Li 2018; Stuedlein et al. 2012; Tietje et al. 2013; Vanmarcke 1977a, 1977b).

Last but not least, the availability of different kind of site-specific soil investigations varies from project to project and layer to layer, and this generally requires a practical approach. Hence there is a gap between the theoretical framework and daily project application.

### 1.1 Outline

This paper addresses the geo-statistical challenges engineers are often confronted with and shows three ways to close the gap between theory and practice. The flow chart presented in Figure 1 illustrates the challenges and their associated sources of uncertainty. For many projects CPTs are the starting point for geotechnical parameter selection. The first part (Ch2) addresses the inherent variation for a single CPT and how this can be related to the Eurocode 7 (EN1997-1 2005). The second part (Ch3) addresses the step towards a more systematic and transparent application of multiple correlations. Reference is made to (Van Berkom 2020; Van Berkom et al. 2022) for a more thorough introduction on this topic. The third part (Ch4) shows how site-specific laboratory tests can be used together with CPT based correlations in a Bayesian approach. The last step, not dealt in this paper, is the determination of constitutive model parameters from the posterior updated soil properties.

It is important to distinguish the different sources of uncertainty. The statistical uncertainty (1), measurements errors (2), inherent uncertainty (3) and transformation uncertainty (4) have been previously introduced in (Phoon and Kulhawy 1999a; Phoon and Kulhawy 1999b). This is also illustrated in Figure 1.

Figure 1 includes three other uncertainties. The method uncertainty (5) is referring to the uncertainty associated with the variation between the methods to derive a geotechnical parameter. It applies to the correlations in the context of CPT interpretation, but also applies to the choice of laboratory tests performed. This differs from the transformation uncertainty which originates from the quality of the data-fitting regression analysis. The method uncertainty is shown in Figure 1 at the level of derived parameter.

Finally, the stratigraphic uncertainty (6) is referring to the

uncertainty in allocating the layers and the model uncertainty (7) accounts for the degree of accuracy of a particular constitutive model. These are not discussed in this study.

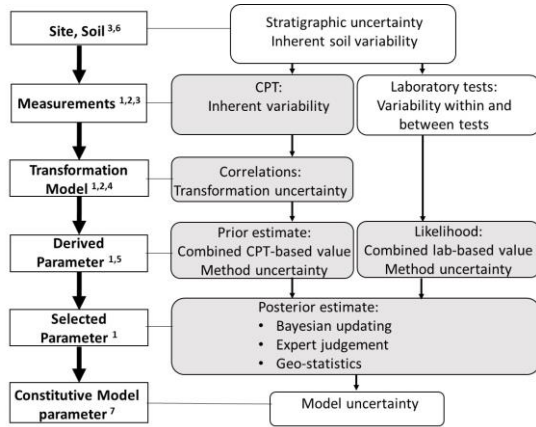


Figure 1: flow chart illustrating the geo-statistical challenges associated with geotechnical parameter determination. Statistical uncertainty (1), measurements errors (2), application of the variance reduction (3). The shaded boxes are topics tackled in this paper.

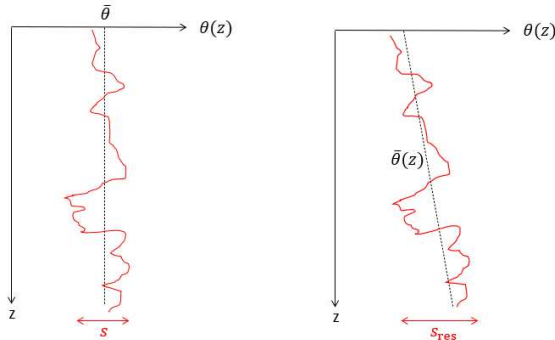


Figure 2: Left: Soil profile with a mean trend not varying with depth, the inherent variability is the empiric standard deviation of the whole data. Right: Soil profile with a mean trend varying with the depth, the inherent variability is the standard error of the residuals

## 2 CPT MEASUREMENTS

### 2.1 Inherent variation

In this section a brief overview has been presented of methods to translate the inherent variation to the representative value for a single CPT. It has also been shown how the characteristic values act as upper and lower bound for the representative value.

The CPT is a type of in-situ test recording the cone resistance  $q_c$ , the sleeve friction  $f_s$  and the pore water pressure  $u_2$  as the cone is pushed into the ground. These variables are typically measured every 2cm, thus providing an almost continuous measurement in the vertical direction. This will allow for stratification into layers based on a soil behavior type classification such as published in (Robertson 2009).

For the sake of generality, we assume in this paper that the variable of interest  $\theta$  is obtained from CPT measurements. We focus in this section on the determination of the inherent variability of the variable  $\theta$  as defined in (Phoon and Kulhawy 1999a; Phoon and Kulhawy 1999b).

In the situation of a single CPT available, only the vertical inherent variability of  $\theta$  is studied, that is to say its variability over the depth in each layer, see Figure 2. If the profile for  $\theta$  does not show a trend varying with the depth (left panel), the empiric standard deviation  $s$  around the mean  $\bar{\theta}$  represents the inherent vertical variability of the variable of interest  $\theta$ . If the profile for  $\theta$  displays an increasing or decreasing trend with the

depth (right panel), a linear regression function can fit the data and the inherent vertical variability is taken as the standard error on regression of the residuals. Alternatively, the inherent variability is also equal to the empirical standard deviation of the detrended profile (Li et al. 2014; Low et al. 2007; Phoon and Kulhawy 1999a; Phoon and Kulhawy 1999b).

### 2.2 Representative value for a single CPT

The Eurocode 7 (EN1997-1 2005) prescribes that the geotechnical parameters shall be based on results derived from laboratory and field tests, complemented by well-established experience and that the characteristic value shall be a cautious estimate of the parameter. In Clause 2.4.5.2(11) of the Eurocode 7 it is stated: “If statistical methods are used, the characteristic value should be derived such that the calculated probability of a worse value governing the occurrence of the limit state under consideration is not greater than 5%.”

In practice both the related terms of characteristic and representative are used for calculations and design. In this paper the following definitions will be used for both terms:

- The characteristic value is statistically defined by the 90% confidence interval. The characteristic value of the population determines the value with 5% confidence level or 95% probability of exceedance (PoE). The characteristic value of the mean of the population determines the mean value with 5% confidence level or 95% probability of exceedance. Hence, these are the definitions of a material property.
- The representative value takes into account the extent of the ground volume involved in the limit state, the effects of stress, state, time, structure and anisotropy. The representative value can be either the characteristic value of the population or of the mean, and any value in between. Hence, this is the definition of a property at the limit state.

The characteristic value of the population for the variable  $\theta$  obtained from  $n$  measurements is determined by the prediction interval as shown in Eq.1, where  $t_{n-1}^{0.95}$  is the Student-t distribution with  $(n-1)$  degrees of freedom for a value with 95% probability of exceedance (PoE). The total variance of the variable  $\theta$  includes both the sample variance  $s^2$  and the variance of the mean  $\sigma_{\bar{\theta}}^2$ , with  $s$  being the empirical standard deviation (see Eq. 2). The variance of the mean (see Eq. 3) is the dispersion of the sample means around the population mean. If one is interested in the characteristic value of the mean, the total variance reduces to the variance of the mean, which yields to Eq. 4. This value corresponds to the confidence interval of the mean.

$$\theta_k = \bar{\theta} - t_{n-1}^{0.95} \sigma_{\theta} \quad (1)$$

$$\sigma_{\theta} = \sqrt{s^2 + s_{\bar{\theta}}^2} = s \sqrt{1 + \frac{1}{n}} \quad (2)$$

$$s_{\bar{\theta}}^2 = s^2/n \quad (3)$$

$$\theta_{k,m} = \bar{\theta} - t_{n-1}^{0.95} s_{\bar{\theta}} = \bar{\theta} - t_{n-1}^{0.95} s \sqrt{\frac{1}{n}} \quad (4)$$

The representative value can be linked to the characteristic boundaries (Eq. 1 and 4). In an attempt to do this, the variance reduction factor  $\Gamma$  as defined by Vanmarcke (1977a, 1977b) can be applied to the sample variance  $s^2$ . The reduction is not applied to variance of the mean  $\sigma_{\bar{\theta}}^2$  as this is the statistical uncertainty related to the sample size. The variance reduction factor is equal to 1 in case the scale of fluctuation is equal or larger than the failure extent. In case the scale of fluctuation is relatively small, the variance reduction factor approaches 0.

The reduced standard deviation accounts for the variance reduction for a specific limit state and soil volume. Hence, the term “representative standard deviation” is introduced which together with the representative value are related to the 5%

confidence level or 95% probability of exceedance (PoE) for the associated limit state in the soil volume of interest (see Eq. 5 and 6).

$$\sigma_{rep} = s \sqrt{\Gamma^2 + \frac{1}{n}} \quad (5)$$

$$\theta_{rep} = \bar{\theta} - t_{n-1}^{0.95} \sigma_{rep} \quad (6)$$

The sampling distance of a CPT is about every 2 cm, whereas the vertical scale of fluctuation is typically one order of magnitude larger. The high sampling rate allows for an accurate determination of the inherent variation by the standard deviation.

Relating the sample size to the number of measurements per layer would give a too high number of samples in Eq.5 for two reasons. First because of the correlation between the measured properties within the scale of fluctuation. The sample size should therefore be estimated based on the layer thickness (D) divided by the vertical scale of fluctuation ( $\delta_v$ ). Second because of not only the cone resistance but in particular the sleeve friction is measured over a larger height, typically 13 cm. As first approximation the scale of fluctuation can be set to typically 0.1 m or the sample size can be set to 10% of the CPT readings per layer.

$$n = \frac{D}{\delta_v} \quad (7)$$

The variance reduction factor is a function of the scale of fluctuation in relation to the extent of failure for a certain limit state. The scale of fluctuation is dominated by geological processes and soil properties whereas the extend of failure is dominated by the geometry and structure dimensions. The variance reduction factor varies between 1 (maximum value) and 0. Various theoretical solutions exist in literature (Ching et al. 2016; Tietje et al. 2013) and a simple approximation is presented in Eq.8.

$$\Gamma^2 = \frac{\delta_v}{D} \quad (8)$$

It is interesting to note that both terms within the square root of Eq.5 are basically very similar. Although these equations can simply be applied to each layer of one CPT, the complexity comes with the determination of the (indirect) geotechnical parameters.

In case the limit state involves a global failure in one layer where all variations are levelled out in the vertical direction, the representative value can be based on the characteristic estimate of the mean. This is in fact an upper bound approach as the only uncertainty that remains is the uncertainty of the mean, related to the sample size (Eq.5). Setting the representative value equal to the characteristic value of the mean is a reasonable assumption for a single CPT as it only considers the averaging of the inherent variation, not of the transformation uncertainty.

Recent random finite element method (RFEM) simulations by (Hicks et al. 2019) confirms that the representative value is indeed bounded by the characteristic values  $\theta_k < \theta_{rep} < \theta_{k,m}$ , hence, for local failures and low variance reduction the representative can be set to the characteristic value. It also showed for the underlying distribution that the equivalent mean is reduced too. This could well be explained by the fact that, despite the averaging process, the limit state is also governed by the weakest path. Reduction of the representative mean is not common practice in engineering. For semi-probabilistic design this would imply that the representative value is likely to be lower than the characteristic value of the mean. For probabilistic design this means that the average should be reduced.

Care should be taken when the limit state involves multiple layers. In a multilayer stratification the height of a single layer is limited allowing for less variance reduction, in particular when

the vertical scale of fluctuation and the layer thickness are similar. Limit states involving multiple layers tend to move more towards a serial system compared to limit states in single layer which are dominated by a parallel system. Unique soil parameters like the friction angle of subsequent layers are likely not correlated, while state parameters such as the pre-overburden stress are likely correlated. Hence, parameters like the undrained shear strength are semi correlated between the layers.

### 3 FROM MEASUREMENTS TO DESIGN PARAMETERS

#### 3.1 An automated framework for parameter determination

In this section the step after performing CPT tests has been presented. For each CPT parameter, both the mean and representative standard deviation related to the inherent variation in each layer are used as input parameters This is combined in the APD framework with the transformation uncertainties for each correlation. The outcome is a set of geotechnical parameters, each with a probability density function.

The necessary design parameters for numerical analysis are not directly measured by in-situ tests. The usage of transformation functions is required to translate the measured variable  $\theta$  into the design property that will be used by the engineer. Most of these transformation functions are correlations obtained from a regression analysis based on empirical data, and therefore introduce an additional source of uncertainty (Phoon and Kulhawy 1999a; Phoon and Kulhawy 1999b). Many correlations have been proposed in the geotechnical engineering literature to derive soil properties and parameters of constitutive models; the outcome for the design parameters may vary significantly depending on which correlation is used. Several of these transformation models can be used successively in series, which makes the determination of the design parameters even more intricate. A proof of concept has been proposed by van Berkomp (Van Berkomp 2020; Van Berkomp et al. 2022) to create system generating paths between the measured variables of a CPT and the desired design properties, based on a given set of correlations. This system called Automatic Parameter Determination (ADP) introduced by Brinkgreve (2019) is based on elements from “graph theory” and enables the visualization of the different paths and the calculation of the destination parameter for each of these paths.

A conceptual example of the graph generated by APD is displayed in Figure 5. A distinction is made between the source nodes of the graph  $\theta_1$  and  $\theta_2$  which usually correspond to the measured variables from in-situ tests ( $q_c, f_s, \dots$ ), and the intermediate and destination nodes  $\omega_1$  and  $\omega_2$  that represent the soil properties obtained from the correlations (i.e. friction angle  $\varphi, \dots$ ). This simple case shows two different paths or possibilities to derive the parameter  $\omega_1$ , and 3 paths to derive the final design parameter  $\omega_2$ .

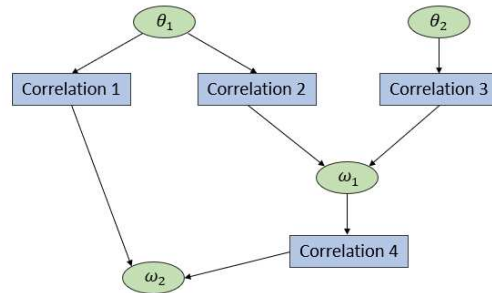


Figure 5: Simple example of a graph generated by APD. The green round nodes representing the parameters are distinguished from the rectangular blue nodes representing the transformation functions.



### 3.2 Input of the framework

The APD framework requires a set of correlations and parameters to generate the graph and the paths. These correlations must come from a thorough review of the literature and should be appropriate to the case study site considered by the engineer. Considerations like the type of soil or the state of consolidation are of importance. In order to perform calculations and propagate them through the network, a mean value and a standard deviation must be introduced for every source parameter of the graph. These two statistics are in practice directly derived from the CPT profiles according to the method proposed in Eq.1-6 (single CPT). Combining the inherent and transformation uncertainty as well as the propagation of the uncertainty through the system is implemented by the First Order Second Moment (FOSM) method. FOSM relies on the linearization of the transformation function using Taylor-series expansion. Phoon and Kulhawy (1999a); (Phoon and Kulhawy 1999b) explain thoroughly how this principle is applied to various geotechnical correlations.

### 3.3 Output of the framework

The mean value and standard deviation for every path of the design parameter are returned as outputs of the APD system. Based on this information and using an appropriate probability distribution (PDF), the user of the system could select the characteristic value that he judges most suitable. An alternative automatic method consists in merging the several contributing distributions into a single combined distribution. As an example, the 3 paths to derive the parameter  $\omega_2$  from the network in Figure 5 are represented by the three contributing distributions displayed in Figure 6.

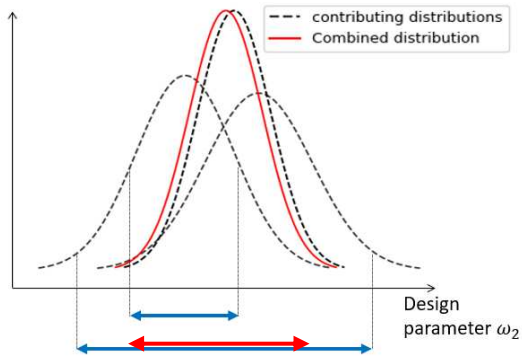


Figure 6: Three contributing normal distribution are combined into a single averaged distribution. The smaller arrow directly relates to the inherent and transformation uncertainty of one path, while the larger arrow accounts for the method uncertainty related to the variety of all correlations (paths). The red arrow illustrates the combined uncertainty of the proposed method.

The combined mean is obtained from a weighted average of the means of each contributing path. The weights are defined as the normalized inverse variance of each path, and the sum of the weights is 1.

$$\bar{x} = \sum_{i=1}^m w_{x,i} x_i \quad (9)$$

$$w_{x,i} = \frac{\frac{1}{\sigma_{x,i}^2}}{\sum_{i=1}^m \frac{1}{\sigma_{x,i}^2}} \quad (10)$$

The combined variance is calculated following the “Propagation method” introduced by (Dormann et al. 2018), which considers the Mean Square Error of the combined mean. Propagation allows the contributing models to be biased but assumes that the averaged prediction  $\bar{x}$  defined in Eq.9 is an unbiased estimator of the true value. This hypothesis is reasonable for bi-directional bias, that is to say a situation where

the individual predictions are spread equally around the true value. Conversely, a uni-directional bias situation would occur when contributing models would consistently underestimate or overestimate the true value. Furthermore it is assumed that all the paths are mutually independent (Hauth 2020). The averaged variance consisting of a bias term and weighted variance term becomes then:

$$var(x) = \left( \sum_{i=1}^m w_{x,i} (x_i - \bar{x}) \right)^2 + \left( \sum_{i=1}^m w_{x,i}^2 \sigma_{x,i}^2 \right) \quad (11)$$

This combined variance accounts for the method uncertainty as well as the inherent and transformation uncertainties. In contrast with the contributing distributions which comprise only the last two sources and for which the respective variances are summed up, the combined distribution incorporates the method uncertainty in a different manner. Its contribution is not summed to the other sources but is instead included in the weighted averaging process. For simplification purposes, the weights are defined as the normalized inverse variance of each path, and all the probability densities are assumed normally distributed.

It is worth noting that the approach adopted to combine distributions is quite general and not restricted to CPT-based outcomes. The same Propagation method can be applied for distributions coming from different type of laboratory tests, to account for the variability between the different types of tests.

## 4 COMBINING CPT CORRELATION AND LOCAL DATA

Although CPT based parameter determination is powerful and provides significant more measurements that often acquainted by laboratory tests, one still need to consider that the correlations can be biased for the specific site and have a limited range of application. In the occasion where some data is available the challenge is how to combine this with the derived values from correlations, such as by APD. This will be shown below.

In case site specific laboratory test data on parameter X is available one can combine these measurements with the results from APD. This is particularly useful in case of few measurements with a relative high variation. The prior density distribution is based on APD and follows a normal distribution  $N(\mu_{X,1}, s_{X,1})$ . The standard deviation of the mean is in line with Eq. 3 defined as  $s_{\bar{x},1} = s_{X,1}/\sqrt{n_1}$  where  $n_1$  is the number of paths (i.e., correlations). Expert judgment can be used alternatively as prior knowledge.

The likelihood PDF is obtained from  $n_2$  direct measurements and follows a normal distribution  $N(\mu_{X,2}, s_{X,2})$ . The use of Bayes' theorem enables the updating of the prior distribution into a posterior distribution based on the information provided by the likelihood.

The posterior mean  $\hat{\mu}_{\bar{x}}$ , posterior standard deviation of the mean  $\hat{s}_{\bar{x}}$ , posterior of the sample standard deviation  $\hat{s}_X$ , and the posterior standard deviation  $\hat{\sigma}_X$  are presented in Eq. 12 to Eq.15:

$$\hat{\mu}_{\bar{x}} = \frac{\mu_{X,1} \cdot s_{X,2}^2 / n_2 + \mu_{X,2} \cdot s_{X,1}^2}{s_{\bar{x},1}^2 + s_{X,2}^2 / n_2} \quad (12)$$

$$\hat{s}_{\bar{x}} = \sqrt{\frac{s_{X,1}^2 \cdot s_{X,2}^2 / n_2}{s_{\bar{x},1}^2 + s_{X,2}^2 / n_2}} \quad (13)$$

$$\hat{s}_X = \sqrt{\frac{s_{X,1}^2 \cdot s_{X,2}^2}{s_{X,1}^2 + s_{X,2}^2}} \quad (14)$$

$$\hat{\sigma}_X = \sqrt{\hat{s}_X^2 + \hat{s}_{\bar{x}}^2} \quad (15)$$

The Eq.12 and Eq.13 originate from (Tang 1971) and have been widely reused by following authors (Orr 2016; Schneider and Schneider 2012). This paper proposes an extension of the concept to update the sample standard deviation (Eq. 14, 15). These posterior standard deviations are in fact equivalent to the “convolution” of the prior and the likelihood distributions,

weighted by their respective normalized inverse squared sample standard deviation. The convolution, being a linear combination of two normal distributions, is also itself a normal distribution (Dormann et al. 2018). With this procedure, both the standard deviation of the mean  $\hat{s}_{\bar{x}}$  and the standard deviation of the  $\hat{s}_x$  are being updated with the likelihood function. This approach slightly differs from (Juang and Zhang 2017) in which only the standard deviation of the mean is being updated.

#### 4.1 Example: Updating the friction angle

We are interested in the determination of the friction angle based on both CPT interpretation and local direct measurements obtained on site. The procedure described in section 2 and the APD system have been applied to derive the combined distribution for the friction angle for 4 different paths as shown in Table 1 and Figure 7 (assumed in this example). The average  $\bar{x} = 38.0$ , the weighted average  $\bar{x} = 37.0$  results from Eq.9 and the combined variance  $var(x) = 6.91$  results from Eq.11. The prior distribution parameters are presented in Table 2 and Figure 7.

Table 1. Example of 4 APD paths.

Path	$\mu_x (^{\circ})$	$s_x (^{\circ})$	$w$	$bias (^{\circ})$
A	34.5	2.0	0.45	3.5
B	38.9	4.0	0.11	0.9
C	38.7	2.5	0.29	0.7
D	39.9	3.5	0.15	1.9

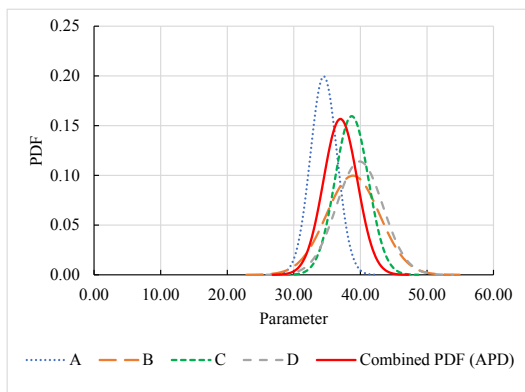


Figure 7: Illustration of PDF's from 4 paths and the combined PDF following the "Propagation method".

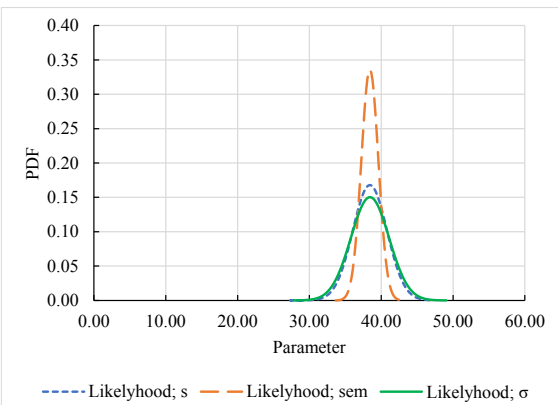


Figure 8: The PDF based on the sample standard deviation (Likelihood; s), the standard deviation of the mean (Likelihood; sem) and overall standard deviation of the distribution (Likelihood;  $\sigma$ ).

Additionally, the friction angle has been obtained from 4 triaxial tests (38.5°, 39.5°, 40.6°, 35.1°), assumed in this example. The likelihood distribution parameters are presented in Table 2

and shown in Figure 8. The characteristic value of the friction angle is derived from Eq. 1 and Eq.2, for the likelihood its value is  $X_k = \mu_{x,2} - 2.35 \sqrt{2.38^2 + 1.19^2} = 32.17^{\circ}$ . The posterior mean value of the friction angle is  $\hat{\mu}_{\bar{x}} = 38.17^{\circ}$ , which is in between the prior and likelihood value. The posterior standard deviation of the mean obtained from Eq.13 is  $\hat{s}_{\bar{x}} = 0.54^{\circ}$ , which is lower than the prior and likelihood value. The posterior sample standard deviation obtained from Eq.14 is  $\hat{s}_x = 1.74^{\circ}$ , which is also lower than the prior and likelihood value. The posterior standard deviation of the friction angle calculated according to Eq.15 is  $\hat{\sigma}_x = \sqrt{1.74^2 + 0.54^2} = 1.82^{\circ}$ . This is the value that should be used when performing a full- or semi-probabilistic analysis and in reliability-based design. This value of the posterior standard deviation includes the statistical uncertainties of the mean and the sample of both the correlations and laboratory tests. The PDF of the prior, likelihood and posterior distribution are illustrated in Figure 9. It is important not to use the value from Eq. 13 as this is the posterior standard deviation of the mean, which would be unsafe as this is a lower value, see Figure 10.

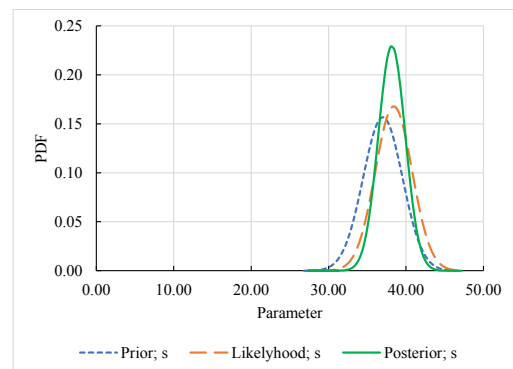


Figure 9: The PDF based on the prior distribution (Prior), the sample distribution (Likelihood) and posterior distribution (Posterior).

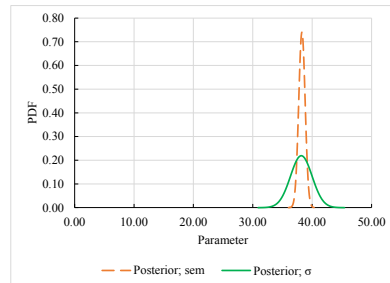


Figure 10: The posterior PDF based on the standard deviation of the mean (Posterior; sem) and the overall standard deviation of the population (Posterior;  $\sigma$ ).

Table 2. Summary of the statistics for the example of Bayesian updating applied to the friction angle.

	$\mu_x (^{\circ})$	$s_x (^{\circ})$	$sem_x (^{\circ})$	$\sigma_x (^{\circ})$	$n$	$t$	$X_k (^{\circ})$
Prior	37.00	2.55	1.27	2.85	4	2.35	30.31
Likelihood	38.43	2.38	1.19	2.66	4	2.35	32.17
Posterior	38.17	1.74	0.54	1.82	4	2.35	33.89
Posterior	38.17	1.74	0.54	1.82	>>	1.65	35.18

An additional assumption must be made for the characteristic value of the posterior as a degree of freedom is required to calculate the Student-t statistics; a cautious estimate recommended by the authors is the number of observations  $n_2$ , alternatively the number of paths from APD into account, see line 4 in Table 2. In case the semi-probabilistic design is based on the

third line in Table 1, using 4 observations, the posterior standard deviation for a full-probabilistic design still needs to be multiplied with a factor (2.35/1.65) to account for the uncertainty in sample size reflected by the Student-t value.

## 5 CONCLUSIONS

This paper addresses the geo-statistical challenges engineers are often confronted with and shows three ways to close the gap between theory and practice. The flow chart presented in Figure 1 illustrates these challenges and their associated sources of uncertainty. For many projects CPTs are the starting point for geotechnical parameter selection. The first part (Ch2) addresses the inherent variation in view of random fields. Methods are presented to derive the representative value for a single CPT and how this can be related to the Eurocode 7 (EN1997-1 2005). The second part (Ch3) addresses the step towards a more systematic and transparent application of multiple correlations. Although this topic is briefly touched, it shows how the inherent and transformation uncertainty is combined with the method uncertainty. The third part (Ch4) shows how site-specific laboratory tests can be used together with CPT based correlations in a Bayesian approach. In the example it is shown how it can be used to determine the posterior mean and standard deviation used in (semi-) probabilistic design.

## 6 ACKNOWLEDGEMENTS

This work is part of the “Perspectief research programme All-Risk” with project number P15-21, which is (partly) financed by NWO Domain Applied and Engineering Sciences.

## 7 REFERENCES

- Brinkgreve, R.B.J. 2019. Automated Model And Parameter Selection: Incorporating Expert Input into Geotechnical Analyses. *Geo-Strata—Geo Institute of ASCE*, **23**(1): 38-45.
- Ching, J., Wu, S.-S., and Phoon, K.-K. 2016. Statistical characterization of random field parameters using frequentist and Bayesian approaches. *Canadian Geotechnical Journal*, **53**(2): 285-298. doi:10.1139/cgj-2015-0094.
- Ching, J., Phoon, K.-K., Chen, K.-F., Orr, T.L.L., and Schneider, H.R. 2020. Statistical determination of multivariate characteristic values for Eurocode 7. *Structural Safety*, **82**: 101893. doi:https://doi.org/10.1016/j.strusafe.2019.101893.
- Dormann, C.F., Calabrese, J.M., Guillera-Aroita, G., Matechou, E., Bahn, V., Bartoń, K., Beale, C.M., Ciuti, S., Elith, J., Gerstner, K., Guelat, J., Keil, P., Lahoz-Monfort, J.J., Pollock, L.J., Reineking, B., Roberts, D.R., Schröder, B., Thuiller, W., Warton, D.I., Wintle, B.A., Wood, S.N., Wüest, R.O., and Hartig, F. 2018. Model averaging in ecology: a review of Bayesian, information-theoretic, and tactical approaches for predictive inference. *Ecological Monographs*, **88**(4): 485-504. doi:https://doi.org/10.1002/ecm.1309.
- Elkateb, T., Chalaturnyk, R., and Robertson, P.K. 2003. An overview of soil heterogeneity: quantification and implications on geotechnical field problems. *Canadian Geotechnical Journal*, **40**(1): 1-15. doi:10.1139/t02-090.
- EN1997-1. 2005. Eurocode 7: Geotechnical design - part 1: General rules. European Committee for Standardization.
- Hauth, M. 2020. Quality assessment of a graph-based approach for a multi-methods determination of geotechnical model parameters. *Civil Engineering and Geosciences*, Delft University of Technology.
- Hicks, M.A., and Nuttall, J.D. Influence of soil heterogeneity on geotechnical performance and uncertainty: a stochastic view on EC7. *In Proceedings 10th International Probabilistic Workshop*, Universität Stuttgart, Stuttgart. 2012. pp. 215-227.
- Hicks, M.A., Varkey, D., van den Eijnden, A.P., de Gast, T., and Vardon, P.J. 2019. On characteristic values and the reliability-based assessment of dykes. *Georisk: Assessment and Management of Risk for Engineered Systems and Geohazards*, **13**(4): 313-319. doi:10.1080/17499518.2019.1652918.
- Juang, C.H., and Zhang, J. 2017. Bayesian Methods for Geotechnical Applications - A Practical Guide. *In Geotechnical Safety and Reliability: Honoring Wilson H. Tang*. pp. 215-246.
- Kulhawy, F.H. On the evaluation of static soil properties. *In Stability and performance of slopes and embankments II*. 1992. ASCE. pp. 95-115.
- Li, D.-Q., Qi, X.-H., Phoon, K.-K., Zhang, L.-M., and Zhou, C.-B. 2014. Effect of spatially variable shear strength parameters with linearly increasing mean trend on reliability of infinite slopes. *Structural Safety*, **49**: 45-55.
- Low, B.K., Lacasse, S., and Nadim, F. 2007. Slope reliability analysis accounting for spatial variation. *Georisk: Assessment and Management of Risk for Engineered Systems and Geohazards*, **1**(4): 177-189. doi:10.1080/17499510701772089.
- Orr, T.L.L. 2016. Defining and selecting characteristic values of geotechnical parameters for designs to Eurocode 7. *Georisk: Assessment and Management of Risk for Engineered Systems and Geohazards*, **11**(1): 103-115. doi:10.1080/17499518.2016.1235711.
- Phoon, K.-K. 2016. Role of reliability calculations in geotechnical design. *Georisk: Assessment and Management of Risk for Engineered Systems and Geohazards*, **11**(1): 4-21. doi:10.1080/17499518.2016.1265653.
- Phoon, K.-K., and Kulhawy, F.H. 1999a. Characterization of geotechnical variability. *Canadian Geotechnical Journal*, **36**(4): 612-624. doi:10.1139/t99-038.
- Phoon, K.-K., and Kulhawy, F.H. 1999b. Evaluation of geotechnical property variability. *Canadian Geotechnical Journal*, **36**(4): 625-639. doi:10.1139/t99-039.
- Prästings, A., Spross, J., and Larsson, S. 2019. Characteristic values of geotechnical parameters in Eurocode 7. *Proceedings of the Institution of Civil Engineers - Geotechnical Engineering*, **172**(4): 301-311. doi:10.1680/jgeen.18.00057.
- Qi, X.-H., and Li, D.-Q. 2018. Effect of spatial variability of shear strength parameters on critical slip surfaces of slopes. *Engineering Geology*, **239**: 41-49. doi:10.1016/j.enggeo.2018.03.007.
- Robertson, P.K. 2009. Interpretation of cone penetration tests — a unified approach. *Canadian Geotechnical Journal*, **46**(11): 1337-1355. doi:10.1139/t09-065.
- Schneider, H.R., and Schneider, M.A. 2012. Dealing with uncertainties in EC7 with emphasis on determination of characteristic soil properties. *Modern Geotechnical Design Codes of Practice* (Arnold P, Fenton GA, Hicks MA and Schweckendiek T (eds)). IOS Press, Rotterdam, the Netherlands: 87-101.
- Stuedlein, A.W., Kramer, S.L., Arduino, P., and Holtz, R.D. 2012. Geotechnical characterization and random field modeling of desiccated clay. *Journal of Geotechnical and Geoenvironmental Engineering*, **138**(11): 1301-1313.
- Tang, W.H. A Bayesian evaluation of information for foundation engineering design. *In 1st International Conference on Applied Statistics and Probability to Soil and Structure Engineering*. Hong Kong 1971. pp. 174-185.
- Tietje, O., Fitze, P., and Schneider, H.R. 2013. Slope Stability Analysis Based on Autocorrelated Shear Strength Parameters. *Geotechnical and Geological Engineering*, **32**(6): 1477-1483. doi:10.1007/s10706-013-9693-8.
- Uzielli, M., Lacasse, S., Nadim, F., and Phoon, K.-K. 2006. Soil variability analysis for geotechnical practice. *Characterization and engineering properties of natural soils*, **3**: 1653-1752.
- Van Berkom, I.E. 2020. An Automated System to Determine Constitutive Model Parameters from In Situ Tests. *Civil Engineering and Geosciences*, Delft University of Technology.
- Van Berkom, I.E., Brinkgreve, R.B.J., Lengkeek, H.J., and De Jong, A.K. 2022. An automated system to determine constitutive model parameters from in situ tests. *In 20th International Conference on Soil Mechanics and Geotechnical Engineering*. Edited by ICSMGE, Sidney. p. 6.
- Vanmarcke, E.H. 1977a. Reliability of earth slopes. *Journal of the geotechnical engineering division*, **103**(11): 1247-1265.
- Vanmarcke, E.H. 1977b. Probabilistic modeling of soil profiles. *Journal of the geotechnical engineering division*, **103**(11): 1227-1246.